Proceedings of the Institute of Acoustics

NUMERICAL COMPARISON OF SOUND FIELD CONTROL STRATEGIES UNDER FREE-FIELD CONDITIONS FOR GIVEN PERFORMANCE CONSTRAINTS

F Olivieri Institute of Sound and Vibration Research, University of Southampton, Southampton, SO17 1BJ, UK.
F M Fazi Institute of Sound and Vibration Research, University of Southampton, Southampton, SO17 1BJ, UK.
M Shin Institute of Sound and Vibration Research, University of Southampton, Southampton, SO17 1BJ, UK.
P A Nelson Institute of Sound and Vibration Research, University of Southampton, Southampton, SO17 1BJ, UK.
S Fontana Huawei European Research Center, Riesstraße 25, 80992, Munich, Germany.
L Yue Huawei European Research Center, Riesstraße 25, 80992, Munich, Germany.

1 INTRODUCTION

Sound Field Control (SFC) is a topic that lies in between Acoustics and Signal Processing (SP) where the aim is to design systems capable of controlling, managing, and manipulating a sound field in a region (or several regions) of the space using an *array* of secondary sources driven by purposefully designed input signals (i.e., complex source strengths).

In order to design the input signals, methods for SFC have been proposed, such as optimal beam-forming, time-reversal signal processing and the pressure-matching method[1–4] as well as methods based on control of the acoustic energy, such as the acoustic contrast maximization[5,6] and the energy difference maximization methods[7,8].

For a given array geometry, techniques for SFC differ between each other based on, for example, the theoretical model and assumptions they rely upon, and on the expressions for the complex source strengths which may depend on various parameters. Due to the aforementioned differences, a "fair" comparison between SFC techniques is not straightforward.

Methods for SFC have been compared in different settings and applications, such as in reflective environments[9], personalized audio in vehicles[10], and generation of warning signals for the safety of pedestrians[11].

In this paper, four SFC methods, i.e. the Delay-and-Sum beam-former, the Pressure-Matching, the Acoustic Contrast Maximization, and the Energy Difference Maximization, have been compared under given constraints on directivity performance and maximum input power to the array by means of computer simulations using a linear array of monopole sources radiating in free-field.

The remainder of the paper is as follows. Section 2 introduces the theoretical background of the four methods for SFC considered in this work. The algorithm for fair comparison of the SFC methods is proposed in Section 3. The simulations and the conclusions are reported in Section 4 and Section 5, respectively.

2 THEORETICAL BACKGROUND

All the acoustical quantities introduced in this section have a time dependence of $e^{j\omega t}$, where $j=\sqrt{-1}$ is the imaginary unit, ω is the angular frequency, and t is time.

With reference to Figure 1, let us consider an array of L sources of coordinates $\mathbf{y}_\ell$, $\ell=1,\ldots,L$, driven by the complex source strengths $\mathbf{q}^T(\omega)=[q_1(\omega),\ldots,q_L(\omega)]$, where $[\cdot]^T$ indicates the operation of vector (or matrix) transpose. The SFC problem in this work is formulated for a control area with a set of M control points of coordinates $\mathbf{x}_m$, $m=1,\cdots,M$ located in the control zone V. The vector of complex sound pressures measured at the control points is $\mathbf{p}^T(\omega)=[p(\mathbf{x}_1,\omega),\ldots,p(\mathbf{x}_M,\omega)]$. Assuming that the superposition of the effects holds in the control zone, the relationship between the sound pressures $\mathbf{p}$ and the source strengths $\mathbf{q}$ can be written as[2]

$$\mathbf{p}(\omega)=\mathbf{Z}(\omega)\,\mathbf{q}(\omega), \tag{1}$$

where

$$\mathbf{Z}_{M\times L}(\omega) = \begin{bmatrix} Z(\mathbf{x}_1,\mathbf{y}_1,\omega) & \cdots & Z(\mathbf{x}_1,\mathbf{y}_L,\omega) \\ \vdots & \ddots & \vdots \\ Z(\mathbf{x}_M,\mathbf{y}_1,\omega) & \cdots & Z(\mathbf{x}_M,\mathbf{y}_L,\omega) \end{bmatrix} \tag{2}$$

is the plant matrix, whose m-th, ℓ-th element is the *electro-acoustical transfer function* between the sound pressures and source strengths. Hereafter, the dependence on the angular frequency ω will be omitted to simplify the notation. The acoustic potential energy density E, hereafter referred to also as acoustic energy, averaged over the M control points is defined as[5,7]

$$E = \frac{1}{M}\|\mathbf{p}\|^2 = \frac{1}{M}\sum_{m=1}^{M}|p(\mathbf{x}_m)|^2 = \frac{1}{M}\mathbf{q}^H\mathbf{Z}^H\mathbf{Z}\mathbf{q} = \mathbf{q}^H\mathbf{R}\mathbf{q}, \tag{3}$$

where $\|\cdot\|^2$ and $|\cdot|$ indicate the operations of l_2-norm squared and absolute value, respectively, and $\mathbf{R} = \frac{1}{M}\mathbf{Z}^H\mathbf{Z}$ represents the spatial correlation of the transfer functions[5,7], and $[\cdot]^H$ indicates the operation of complex conjugate transpose. Similarly, the *input energy* E_q of the array of sources, also referred to as array effort, is defined as

$$E_q = \|\mathbf{q}\|^2 = \mathbf{q}^H\mathbf{q} \tag{4}$$

and it is used as a measure of the input power required by the array to control the sound field[6].

For the SFC problem under consideration, a given control point could be either *acoustically bright* or *acoustically dark*, depending on where the sound pressure level is to be *maximized* or *minimized*, respectively. The coordinates of the bright and dark points are denoted with $\mathbf{x}_b^{(B)}$, $b = 1,\cdots,M_B$ and $\mathbf{x}_d^{(D)}$, $d = 1,\cdots,M_D$, where M_B and M_D are the number of bright and dark points in the control area, respectively, and $M_B + M_D = M$. Using the above notations, the sound pressure $\mathbf{p}_B$, the plant matrix $\mathbf{Z}_B$, and the acoustic potential density energy E_B measured at the control points in the bright zone can be represented as

$$\mathbf{p}_B = \mathbf{Z}_B\mathbf{q}, \qquad \mathbf{Z}_B = \begin{bmatrix} Z(\mathbf{x}_1^{(B)},\mathbf{y}_1) & \cdots & Z(\mathbf{x}_1^{(B)},\mathbf{y}_L) \\ \vdots & \ddots & \vdots \\ Z(\mathbf{x}_{M_B}^{(B)},\mathbf{y}_1) & \cdots & Z(\mathbf{x}_{M_B}^{(B)},\mathbf{y}_L) \end{bmatrix}, \qquad E_B = \mathbf{q}^H\mathbf{R}_B\mathbf{q}, \tag{5}$$

and the same quantities measured at the control points in the dark zone are described by

$$\mathbf{p}_D = \mathbf{Z}_D\mathbf{q}, \qquad \mathbf{Z}_D = \begin{bmatrix} Z(\mathbf{x}_1^{(D)},\mathbf{y}_1) & \cdots & Z(\mathbf{x}_1^{(D)},\mathbf{y}_L) \\ \vdots & \ddots & \vdots \\ Z(\mathbf{x}_{M_D}^{(D)},\mathbf{y}_1) & \cdots & Z(\mathbf{x}_{M_D}^{(D)},\mathbf{y}_L) \end{bmatrix}, \qquad E_D = \mathbf{q}^H\mathbf{R}_D\mathbf{q}, \tag{6}$$

where $\mathbf{R}_B$ and $\mathbf{R}_D$ are the spatial correlation matrices of the bright and dark zones, respectively. The expressions of $\mathbf{p}_D$, $\mathbf{Z}_D$, $\mathbf{p}_B$, and $\mathbf{Z}_B$ relate to $\mathbf{p}$ and $\mathbf{Z}$ through the relationships $\mathbf{p} = \left[\mathbf{p}_B^T\mathbf{p}_D^T\right]^T$ and $\mathbf{Z} = \left[\mathbf{Z}_B^T\mathbf{Z}_D^T\right]^T$[8].

2.1 Methods for Sound Field Control

In this section, the theoretical models of the SFC methods considered in this work are reviewed.

The Delay-and-Sum (DAS) [12] is an algorithm that makes use of delay lines to focus sound in space, wherein the input signals to the array are aligned in time so that they undergo constructive acoustic interference at the bright point. Assuming one control point in the bright zone and by defining $\mathbf{z}_B^T = [Z(\mathbf{x}_1^{(B)},\mathbf{y}_1),\cdots,Z(\mathbf{x}_1^{(B)},\mathbf{y}_L)]$ as the vector of the transfer functions between the sources and the bright point, the expression for the complex source strength calculated with the delay-and-sum method can be written as[11]

$$\mathbf{q}_{DAS} = \frac{\mathbf{z}_B^*}{\mathbf{z}_B^*\mathbf{z}_B}, \tag{7}$$

where $[\cdot]^*$ indicates the operation of complex conjugate.

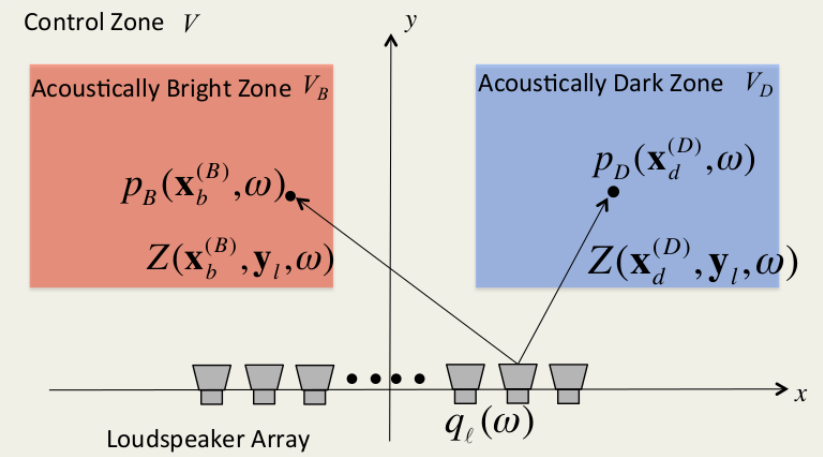

Figure 1: Example of a SFC control problem.

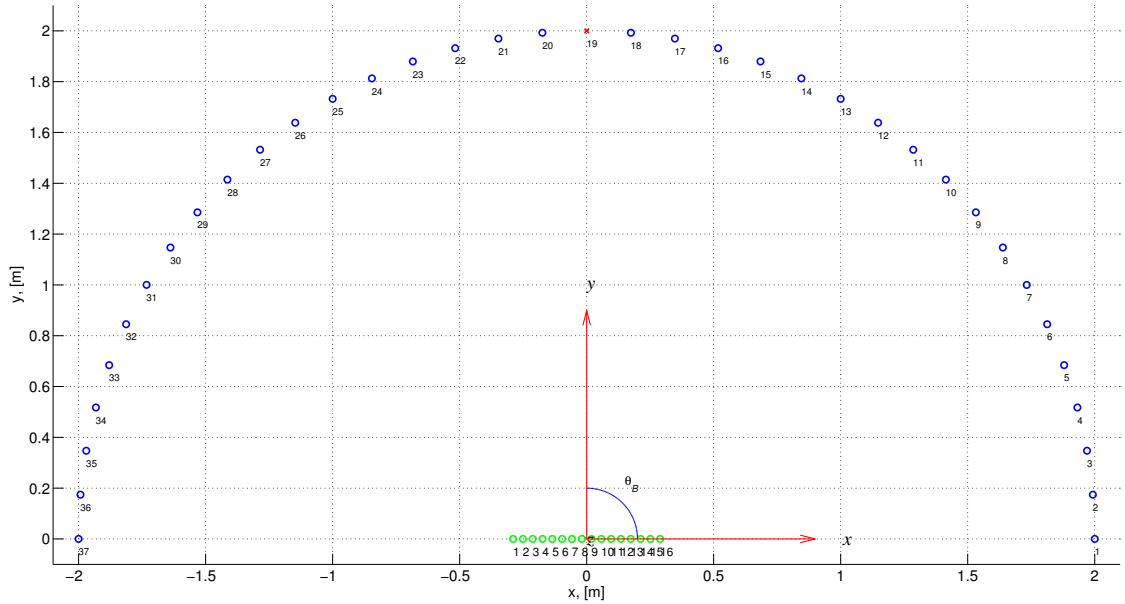

Figure 2: Control zone setup for the linear array - The green, blue, and red circles indicate the sources, the dark points, and the bright point, respectively.

The Pressure-Matching (PM) method [2,13,14] is based on the minimization of the complex error $\mathbf{e}_{\mathrm{PM}} = \hat{\mathbf{p}} - \mathbf{p} = \hat{\mathbf{p}} - \mathbf{Z}\mathbf{q}$, in a least-squares sense, between the desired and arbitrarily chosen *target sound pressures* $\hat{\mathbf{p}}^T = [\hat{p}(\mathbf{x}_1), \ldots, \hat{p}(\mathbf{x}_M)]$ (also called *target signal*) and the reproduced pressure $\mathbf{p}$, both defined at the control points[2,14]. The cost function J_{PM} to be minimized is defined as the sum of the squared reproduction complex error term $\mathbf{e}_{\mathrm{PM}}$, and of an effort penalty term $\beta\mathbf{q}^H\mathbf{q}$, that is[14]

$$J_{\mathrm{PM}} = \mathbf{e}_{\mathrm{PM}}^H\mathbf{e}_{\mathrm{PM}} + \beta_{\mathrm{PM}}\mathbf{q}^H\mathbf{q}, \tag{8}$$

where $\beta_{\mathrm{PM}} \in [0,\infty)$ is the *Tikhonov regularization* parameter, which can be frequency dependent[2,14]. The cost function J_{PM} is convex with respect to the imaginary and real parts of the $\mathbf{q}$ and it has a unique global minimum[13]. The source strength vector $\mathbf{q}_{\mathrm{PM}}$ that minimizes the cost function J_{PM} is found by setting to zero the complex gradient of J_{PM} with respect to $\mathbf{q}$ and then solving with respect to $\mathbf{q}$[14]. Assuming $M > L$, the complex source strength $\mathbf{q}_{\mathrm{PM}}$ is given by[13,14]

$$\mathbf{q}_{\mathrm{PM}} = [\mathbf{Z}^H\mathbf{Z} + \beta_{\mathrm{PM}}\mathbf{I}]^{-1}\mathbf{Z}^H\hat{\mathbf{p}}, \tag{9}$$

where $[\cdot]^{-1}$ indicates the operation of matrix inversion. In this work, the target signal at the control points is defined as $\hat{\mathbf{p}}^T = [\hat{\mathbf{p}}_B^T \hat{\mathbf{p}}_D^T]$, where $\hat{\mathbf{p}}_B^T = [\hat{p}(\mathbf{x}_1^{(B)}), \ldots, \hat{p}(\mathbf{x}_{M_B}^{(B)})]$, $\hat{p}(\mathbf{x}_b^{(B)}) = 1$, and $\hat{\mathbf{p}}_D^T = [\hat{p}(\mathbf{x}_1^{(D)}), \ldots, \hat{p}(\mathbf{x}_{M_D}^{(D)})]$, $\hat{p}(\mathbf{x}_d^{(D)}) = 0$, are the target signals in the bright and dark zone, respectively.

The Acoustic Contrast Maximization (ACM) method was introduced by Choi et al. and it aims at the maximization of the acoustic contrast (AC), which is defined as the ratio between the averaged energy density in the acoustically bright and dark zones, that is[5]

$$\mathrm{AC} = \frac{E_B}{E_D} = \frac{\mathbf{q}^H \mathbf{R}_B \mathbf{q}}{\mathbf{q}^H \mathbf{R}_D \mathbf{q}}, \tag{10}$$

The cost function to be maximized is $J_{ACM} = \mathrm{AC}$ and the source strength vector that maximizes J_{ACM} is given by the following eigenvalue problem[5,6]

$$\lambda_n \mathbf{q}_n = \left(\mathbf{R}_D^{-1} \mathbf{R}_B\right) \mathbf{q}_n, \tag{11}$$

where λ_n is the n-th eigenvalue of matrix $\mathbf{R}_D^{-1}\mathbf{R}_B$.The optimal source strength $\mathbf{q}_{ACM}$ is calculated by selecting the eigenvector corresponding to the maximum eigenvalue of the matrix $[\mathbf{R}_D + \beta_{\mathrm{ACM}}\mathbf{I}]^{-1}\mathbf{R}_B$[5], where the regularization factor $\beta_{\mathrm{ACM}} \in [0, \infty]$ is introduced due to the presence of the operation of matrix inversion.

The Energy difference Maximization (EDM) , proposed by Shin et al., aims at maximizing the acoustic energy difference between the bright and the dark zones. The cost function J_{EDM} to be maximized is defined as[7]

$$J_{\mathrm{EDM}}(\mathbf{q}) = \frac{E_B - \alpha E_D}{E_q} = \frac{\mathbf{q}^H (\mathbf{R}_B - \alpha \mathbf{R}_D) \mathbf{q}}{\mathbf{q}^H \mathbf{q}}, \tag{12}$$

where α is a positive real-valued factor used to adjust the relative importance between acoustic energy difference[7] and the control effort for the energy in the dark zone[8]. The source strength vector is obtained from the following eigenvalue problem[7,8]

$$\lambda_n \mathbf{q}_n = (\mathbf{R}_B - \alpha \mathbf{R}_D) \mathbf{q}_n \tag{13}$$

by selecting the eigenvector corresponding to the maximum eigenvalue of the matrix $\mathbf{R}_B - \alpha \mathbf{R}_D$. It is important to emphasize that the solution of the EDM method does not involve the operation of matrix inversion.

2.2 Performance evaluation

In this work, performance of the SFC algorithms are evaluated in terms of Acoustic Contrast (defined in Eqn. (10)), Array Efficiency ($A\hat{E}$), and directivity patterns.

Let p_B be the sound pressure measured at the bright point due to the array driven by the complex source strength $\mathbf{q}$. Let E_{LMON} be the input energy required to L monopoles, co-located at the acoustic center of the array and operating in phase, to generate p_B at the bright point. The Array Efficiency ($A\hat{E}$) is defined as the ratio between E_{LMON} and the input energy E_q, that is

$$A\hat{E} = 10\log_{10}\left(\frac{E_{LMON}}{E_q}\right) = 10\log_{10}\left(\frac{(4\pi r_B)^2 |p_B|^2}{E_q}\right), \tag{14}$$

where r_B is the radial coordinate of the bright point given in polar coordinates. The performance parameters have been averaged in six frequency bands with uniform frequency spacing defined by the following ranges $[177, 355]Hz$, $[355, 710]Hz$, $[710, 1420]Hz$, $[1420, 2840]Hz$, $[2840, 5680]Hz$, $[5680, 11360]Hz$. The center frequencies corresponding to the given frequency bands are $[250, 500, 1000, 2000, 4000, 8000]Hz$.

3 STRATEGY FOR FAIR COMPARISON OF ALGORITHMS FOR SFC

For a given array geometry and a given set-up of the control zone, the considered algorithms for SFC require to set the values of *tuning parameters*, such as the regularization factors β_{PM} and β_{ACM} in the PM and ACM methods, and α in the EDM method. Those parameters have, in general, a significant impact on the performance of algorithm for SFC. For example, the regularization factor β_{PM} in the PM method controls the trade-off between the directional performance and the input power required by the array whereas the regularization factor β_{ACM} in the ACM method *does not* control the input power[8]. The tuning factor α controls the energy difference between the bright and the dark zones[8].

In order to compare the algorithms, two performance constraints - on the maximum input power to the array and to the reconstructed pressure at the bright point - are introduced. The tuning parameters are then used along with a compensation filter to satisfy the performance constraints.

Magnitude and phase compensation of the pressure at a chosen bright point The first constraint is set to ensure that the calculated complex source strengths $\mathbf{q}$ provide for the perfect reconstruction of a target signal $\hat{p}_b$, where b is the index of a bright point chosen from the set of M_B points in the bright zone. Whilst the PM method allows for the control of the magnitude and phase of the reconstructed pressure at the control points, methods based on the control of the acoustic energy do not allow to control the phase of the sound pressure at the control points[8]. Due to this fact, Shin et al have proposed a "phase-compensation" filter applied to the source strengths obtained with the EDM method to match the phase of the reconstructed pressure at a given point in the bright area with that of the target pressure at the the same point[8]. In principle, the compensation filter can also be applied to the ACM method. Using a similar concept as the "phase-compensation" filter, a filter W_{MPC} for compensation of the *magnitude and phase* of the reconstructed pressure p_b with respect to a desired target signal $\hat{p}_b$ is proposed to implement the constraint on the reconstructed pressure at the bright point. The filter is applied to the $\mathbf{q}$ designed with a given algorithm, thus giving the *compensated source strengths* $\hat{\mathbf{q}}$ defined as

$$\hat{\mathbf{q}} = W_{\mathrm{MPC}}\mathbf{q}, \tag{15}$$

where W_{MPC} is the MPC (Magnitude and Phase Compensation) filter and it is defined as

$$W_{\mathrm{MPC}} = \frac{\hat{p}_b}{p_b} = \frac{\hat{p}_b}{\mathbf{z}_b^T\mathbf{q}}. \tag{16}$$

The constraint can be written as

$$\text{Constraint 1} : p_b(\hat{\mathbf{q}}) = \hat{p}_b. \tag{17}$$

Limit on the Input Power The second constraint is set to ensure that the input power to the array $\|\hat{\mathbf{q}}\|^2 = \sum_{\ell=1}^{L} |\hat{q}_\ell|^2$ driven with the compensated source strengths does not exceed a given maximum value $\|\mathbf{q}\|^2_{\mathrm{MAX}}$. This can be written as

$$\text{Constraint 2} : \|\hat{\mathbf{q}}\|^2 \leq \|\mathbf{q}\|^2_{\mathrm{MAX}}. \tag{18}$$

In this paper, $\|\mathbf{q}\|^2_{\mathrm{MAX}}$ is expressed in terms of the input power required by L monopoles radiating in free-field and operating in phase that are focusing sound at one bright point located at $\mathbf{x}_B$ and producing the sound pressure $p_B = 1$. Let the distance between the bright point and each monopole be equal to r_ℓ. By assuming $r_\ell \approx R$, the *reference input power* $\|\mathbf{q}\|^2_{ref}$ can be written as

$$\|\mathbf{q}\|^2_{ref} = \sum_{\ell=1}^{L} \left(\frac{4\pi R}{L}\right)^2 = \left(\frac{4\pi R}{\sqrt{L}}\right)^2. \tag{19}$$

However, for a given SFC method, the above value for the reference input power might be quite a restrictive limit, especially at low frequency. Therefore, $\|\mathbf{q}\|^2_{\mathrm{MAX}}$ has been defined as

$$\|\mathbf{q}\|^2_{\mathrm{MAX}} = \sigma \|\mathbf{q}\|^2_{ref}, \tag{20}$$

INPUTS = ε_β, σ, $\|\mathbf{q}\|^2_{ref}$, β_{MIN}.
Calculate $\|\mathbf{q}\|^2_{\text{MAX}}$ (Eqn. (20))
Initialize $\beta = \beta_{\text{MIN}}$
Calculate $\mathbf{q}$ using PM or ACM
Calculate $\hat{\mathbf{q}} = W_{\text{MPC}}\mathbf{q}$
while $\|\hat{\mathbf{q}}\|^2 > \|\mathbf{q}\|^2_{\text{MAX}}$ **do**
  $\beta = \beta + \varepsilon_\beta$
  Calculate $\mathbf{q}$ using PM or ACM
  Calculate $\hat{\mathbf{q}} = W_{\text{MPC}}\mathbf{q}$
end while

return β, $\hat{\mathbf{q}}$

(a) Procedure to compute β and $\hat{\mathbf{q}}$ for PM and ACM methods.

INPUTS = ε_α, σ, $\|\mathbf{q}\|^2_{ref}$, α_{MAX}.
Calculate $\|\mathbf{q}\|^2_{\text{MAX}}$ (Eqn. (20))
Initialize $\alpha = \alpha_{\text{MAX}}$
Calculate $\mathbf{q}$ using EDM
Calculate $\hat{\mathbf{q}} = W_{\text{MPC}}\mathbf{q}$
while $\|\hat{\mathbf{q}}\|^2 > \|\mathbf{q}\|^2_{\text{MAX}}$ & $\alpha \geq 0$ **do**
  $\alpha = \alpha - \varepsilon_\alpha$
  Calculate $\mathbf{q}$ using EDM
  Calculate $\hat{\mathbf{q}} = W_{\text{MPC}}\mathbf{q}$
end while

return α, $\hat{\mathbf{q}}$

(b) Procedure to compute α and $\hat{\mathbf{q}}$ for EDM method

Alg. 1: Pseudo-code of the algorithms for the implementation of the performance constraints.

where σ is a positive real-valued safety factor. In all the simulations, the safety factor is set to $\sigma = 2.25$. Furthermore, it is assumed that the maximum hard-bound limit to the input power to the array is constant over frequency and equal to $\|\mathbf{q}\|^2_{\text{MAX}}(\omega) = 2.25\,\|\mathbf{q}\|^2_{ref}$. The value of $\|\mathbf{q}\|^2_{\text{MAX}}$ can be expressed in dB with respect to the unitary input voltage to the array of sources.

Implementation of the constraints Having introduced the two performance constraints, an algorithm that makes use of the tuning parameters of the methods along with the MPC filter is introduced and used for fair comparison of the methods. For a given algorithm and a tuning parameter, the approach is to iteratively increase (or decrease) the tuning parameter and calculate the compensated complex source strengths $\hat{\mathbf{q}}$ using Eqn. (15) until they meet the constraint on the maximum input power in Eqn. (18). As a result of this procedure, the compensated source strengths, the compensation filters, and the tuning parameter are obtained. The algorithms to implement the given performance constraints for the PM and ACM methods and for the EDM method are reported in the form of pseudo-codes in Algorithm 1a and Algorithm 1b, respectively. The compensation filters for the Delay-and-sum can be applied directly by substituting Eqn. (7) into Eqn. (15). Although the domain of the regularization factor β for both PM and ACM (i.e., β_{PM} and β_{ACM}) is $[0,\infty)$, in order to ensure a faster convergence of the algorithm, the domain is chosen as $[\beta_{\text{MIN}},\infty)$, where β_{MIN} is the minimum value for the regularization set by the user. The regularization factor is updated, at each iteration i, using the rule $\beta_i = \beta_{i-1} + \varepsilon_\beta$, where ε_β is the step size. Instead, the EDM tuning parameter α is updated using the rule $\alpha_i = \alpha_{i-1} - \varepsilon_\alpha$ from $\alpha = \alpha_{\text{MAX}}$ to $\alpha = 0$, where ε_α is the step size of the EDM parameter. Both the step sizes ε_β and ε_α are set by the user and the role of the choice of a given value for the step size in the calculation of the compensated source strengths is not discussed in this paper. The values of the step sizes and the input parameters to the algorithms used in this paper are defined in the next section.

4 SIMULATIONS

The control zone considered in this set of simulations consists of $M = 37$ control points uniformly arranged on a semi-circle of radius $R = 2$m. The angle between adjacent control points is $5°$. A single bright point is chosen, located at $\theta_B = 90°$, where θ_B is the angle of the bright point given in polar coordinates. The other $M_D = 36$ control points are set as dark points. The array of sources consists of $L = 16$ equally-spaced sources arranged in a linear geometry. The spacing between adjacent sources is $d = 3.86$cm. The coordinate of the ℓ-th transducer of the array is given by $\mathbf{y}_\ell = [\ell d/2, 0]^T$, where $\ell \in [-(L-1), L-1]$. Figure 2 shows the sound field control setup considered in this paper and indicates the location of the sources and of the bright and dark points. The sampling frequency is set to $f_s = 48$ kHz. If the sources of the array radiate sound as ideal monopole sources in free-field, then

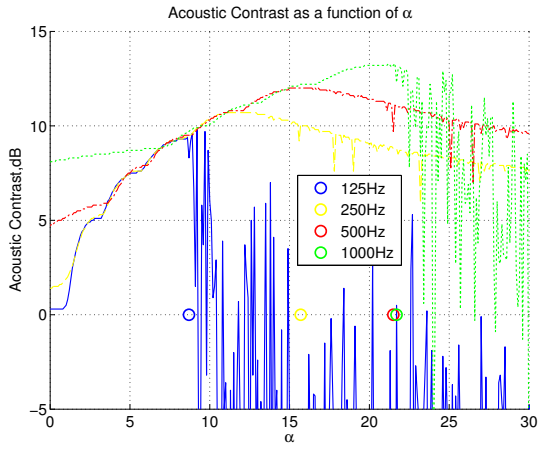

Figure 3: Acoustic Contrast as a function of α_{MAX} - Single frequencies.The circles indicate the selected values of α_{MAX} at each frequency.

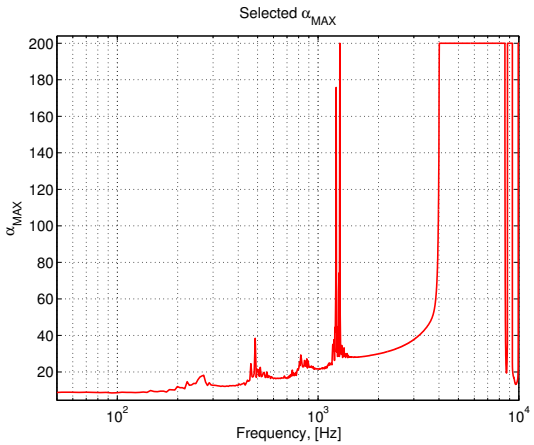

Figure 4: Selected EDM α_{max} as a function of frequency.

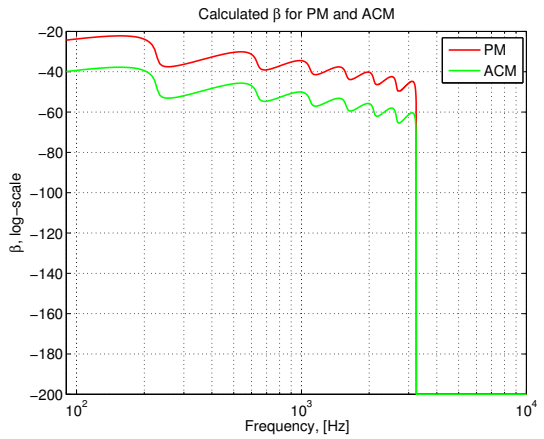

Figure 5: Calculated regularization factors.

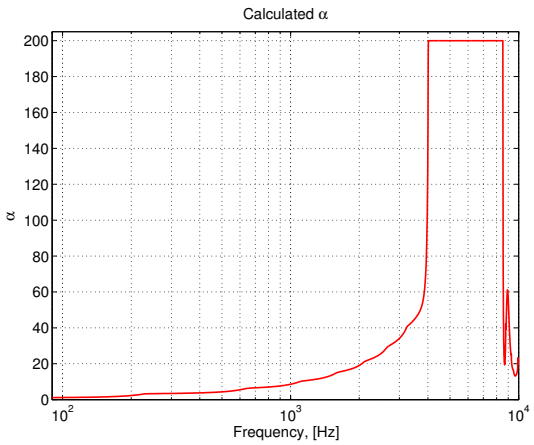

Figure 6: Calculated α.

the elements of the plant matrix can be expressed as

$$Z(\mathbf{x}_m, \mathbf{y}_\ell, \omega) = \frac{e^{-j\frac{\omega}{c}|\mathbf{x}_m - \mathbf{y}_\ell|}}{4\pi|\mathbf{x}_m - \mathbf{y}_\ell|}, \tag{21}$$

where $|\mathbf{x}_m - \mathbf{y}_\ell|$ is the distance between the two vectors $\mathbf{x}_m$ and $\mathbf{y}_\ell$.

The values of the parameters used in Algorithm 1a for the PM method are $\varepsilon_\beta^{PM} = 10^{-6}$ and $\beta_{\mathrm{MIN}}^{PM} = 10^{-20}$. Those used for the ACM method are $\varepsilon_\beta^{ACM} = 10^{-9}$ and $\beta_{\mathrm{MIN}}^{ACM} = 10^{-20}$. The step size for Algorithm 1b is $\varepsilon_\alpha = 10^{-2}$. The value of α_{MAX} has been calculated as described next. Figure 3 shows the acoustic contrast (in dB) as a function of $0 < \alpha < 200$ and the MPC filter at five frequencies $[125, 250, 500, 1000]Hz$. As shown by these results, the AC increases quite smoothly up to a certain value of α and then it starts decreasing and becomes more erratic. Assuming that the AC increases smoothly up to a given value of alpha, then α_{MAX} is selected as the value of α for which the second derivative of AC in absolute value does not exceed a given threshold in dB, which, in this simulations, is set to 0.01 dB. The circles in Figure 3 show the value of α_{MAX} selected with the proposed procedure at the frequencies considered and Figure 4 shows the selected EDM α_{MAX} as a function of frequency.

Figure 7 shows the perfect overlap between the responses of the reconstructed pressure at the bright point due to the compensated source strengths for all the algorithms considered. This indicates that the second constraint is fulfilled in all the cases.

The regularization factors for the PM and ACM methods and α calculated with the proposed algorithms are shown in Figure 5 and Figure 6, respectively. The magnitude and phase responses of the compensation filters for all the algorithms are shown in Figure 8 and Figure 9, respectively. The compensation filter for the DAS has constant magnitude whilst the W_{MPC} for the PM method is a frequency-dependent gain. The W_{MPC} for the ACM can be almost regarded as a low-pass filter with cut-off frequency at 3 kHz and linear phase response. This is similar to the compensation filter for the EDM, although the magnitude response after 8 kHz becomes more erratic and the phase response is not linear and this might lead to non-constant group delay.

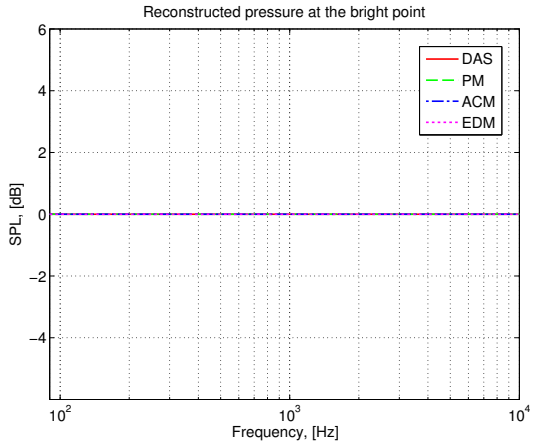

Figure 7: Reconstructed pressure at the bright point.

The frequency-averaged directivity patterns for six frequency bands for the four algorithms considered obtained with the proposed strategy are shown in Figure 10. At low frequencies, the DAS method shows the poorest performance in terms of directivity. The PM and ACM are quite similar at all frequencies. The EDM also shows the same performance as PM and ACM for all the frequency bands apart from frequency band number 6, wherein the level of the side-lobes is higher than the other algorithms.

The Acoustic Contrast averaged in frequency bands is shown in Figure 11. The DAS method shows lower AC with respect to the other equalized complex source strengths designed with PM, ACM, and EDM.

The Array Efficiency averaged in six frequency bands is shown in Figure 12. The DAS exhibits the highest efficiency. Apart from low frequency, where the PM, ACM, and EDM methods show similar values of efficiency, at high frequency the EDM has lower performance with respect to the PM and ACM.

5 CONCLUSIONS

In this paper, four widely used methods for Sound Field Control have been compared by means of computer simulations under free-field conditions. For a given array geometry and control zone set-up, the performance of these methods depend on tuning parameters. In order to enable a fair comparison between methods, a signal processing strategy to implement performance constraints on maximum input power to the array and on the reconstructed pressure at the bright point has been

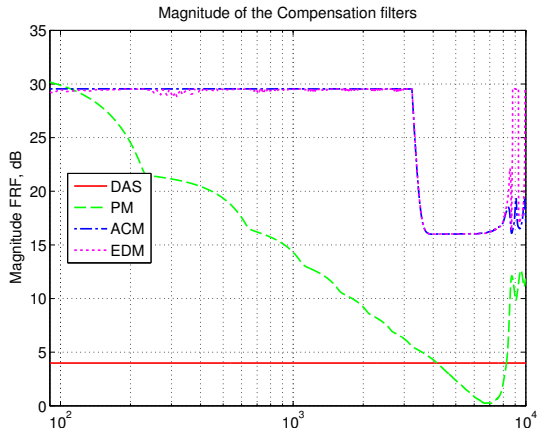

Figure 8: Magnitude FRF response of compensation filters

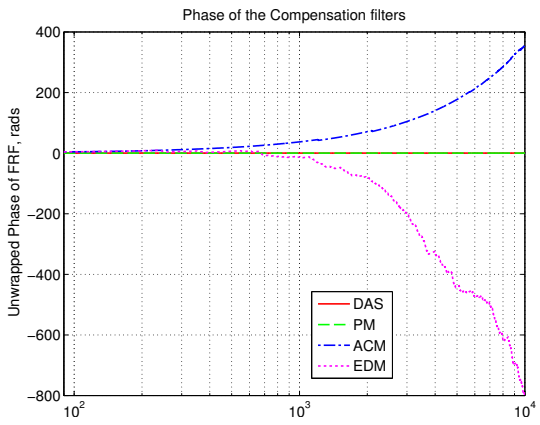

Figure 9: Phase FRF response of compensation filters

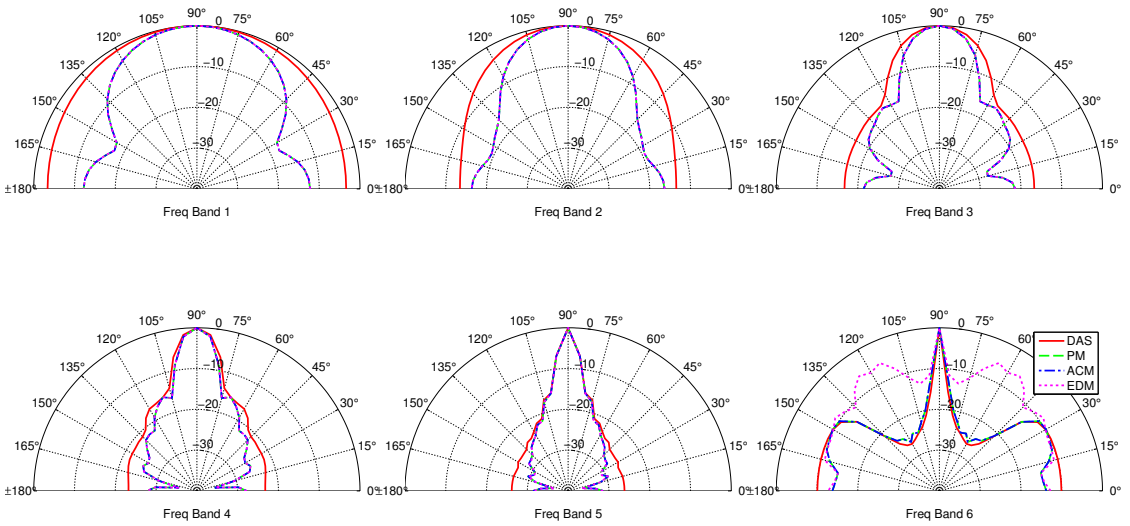

Figure 10: Directivity Patterns of the compensated source strengths averaged in frequency bands. The radial and angular coordinates are given in dB re 1 [Pa] and in degrees, respectively.

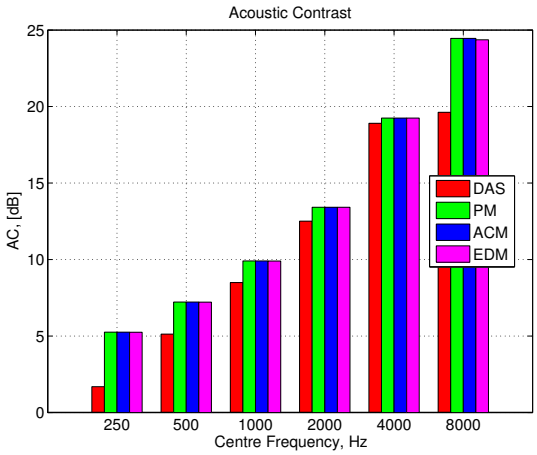

Figure 11: Acoustic Contrast in frequency bands.

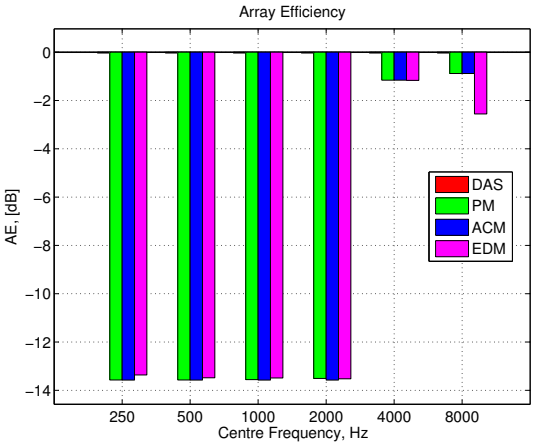

Figure 12: Array Efficiency in frequency bands.

proposed and applied to the considered SFC methods. The strategy allows for the calculation of the tuning parameters and of a filter for the perfect reconstruction of a target signal defined at the bright point, thus returning the compensated source strengths which fulfill the performance constraints. The compensated source strengths have then been compared in terms of acoustic contrast, array efficiency, and directivity patterns. For the given array and control zone setup, simulations have shown that, at low frequencies, the compensated source strengths of the PM, ACM, and EDM methods can reach almost identical performance in terms of all the parameters considered. The compensated DAS shows the lowest contrast and poorest directivity performance but the highest efficiency. At high frequencies, the compensated source strengths calculated with the PM and ACM methods show slightly higher acoustic contrast than the ones calculated with the EDM method. Differences in array efficiency between the compensated PM, ACM, and EDM are more significant at high frequencies, where the efficiency of the PM and ACM method is higher than that of the compensated EDM.

References

[1] H. Cox, R. Zeskind, and T. Kooij, "Practical supergain," *IEEE Transactions on Acoustics, Speech, and Signal Processing*, vol. 34, no. 3, pp. 393–398, Jun. 1986.

[2] O. Kirkeby and P. Nelson, "Reproduction of a plane wave sound fields," *The Journal of the Acoustical Society of America*, vol. 4, no. November, pp. 2992–3000, 1993.

[3] M. Tanter, J. L. Thomas, and M. Fink, "Time reversal and the inverse filter." *The Journal of the Acoustical Society of America*, vol. 108, no. 1, pp. 223–34, Jul. 2000.

[4] J. H. Chang and F. Jacobsen, "Sound field control with a circular double-layer array of loudspeakers," *The Journal of the Acoustical Society of America*, vol. 131, no. 6, p. 4518, Jun. 2012.

[5] J. W. Choi and Y. H. Kim, "Generation of an acoustically bright zone with an illuminated region using multiple sources," *The Journal of the Acoustical Society of America*, vol. 111, no. 4, p. 1695, 2002.

[6] S. J. Elliott, J. Cheer, J. W. Choi, and Y. Kim, "Robustness and Regularization of Personal Audio Systems," *IEEE Transactions on Audio, Speech, and Language Processing*, vol. 20, no. 7, pp. 2123–2133, Sep. 2012.

[7] M. Shin, S. Q. Lee, F. M. Fazi, P. A. Nelson, D. Kim, S. Wang, K. H. Park, and J. Seo, "Maximization of acoustic energy difference between two spaces," *The Journal of the Acoustical Society of America*, vol. 128, no. 1, pp. 121–31, Jul. 2010.

[8] M. Shin, F. M. Fazi, P. A. Nelson, and F. C. Hirono, "Controlled sound field with a dual layer loudspeaker array," *Journal of Sound and Vibration*, vol. 333, no. 16, pp. 3794–3817, Aug. 2014.

[9] M. Olik, J. Francombe, P. Coleman, P. J. B. Jackson, M. Olsen, M. Moller, and S. Bech, "A Comparative Performance Study of Sound Zoning Methods in a Reflective Environment," in *Audio Engineering Society Conference: 52nd International Conference: Sound Field Control - Engineering and Perception*, Guildford, UK, Sep. 2013.

[10] J. Cheer and S. J. Elliott, "A Comparison of Control Strategies for a Car Cabin Personal Audio System," in *Audio Engineering Society Conference: 52nd International Conference: Sound Field Control - Engineering and Perception*, Guildford, UK, Sep. 2013.

[11] A. Berkhoff and R. V. D. Rots, "Directional sound sources using real-time beamforming control," in *42nd International Congress and Exposition on Noise Control Engineering - Noise Control for Quality of Life - INTER-NOISE 2013*, Innsbruck, Austria, Sep. 2013.

[12] J. Benesty, J. Chen, and Y. Huang, *Microphone Array Signal Processing*, ser. Springer topics in signal processing. Springer, 2008.

[13] P. A. Nelson and S. J. Elliott, *Active control of sound*. Academic Press, 1993.

[14] O. Kirkeby, P. A. Nelson, F. Orduna-Bustamante, and H. Hamada, "Local sound field reproduction using digital signal processing," *The Journal of the Acoustical Society of America*, vol. 100, no. 3, p. 1584, 1996.